CHALMERS
UNIVERSITY OF TECHNOLOGY

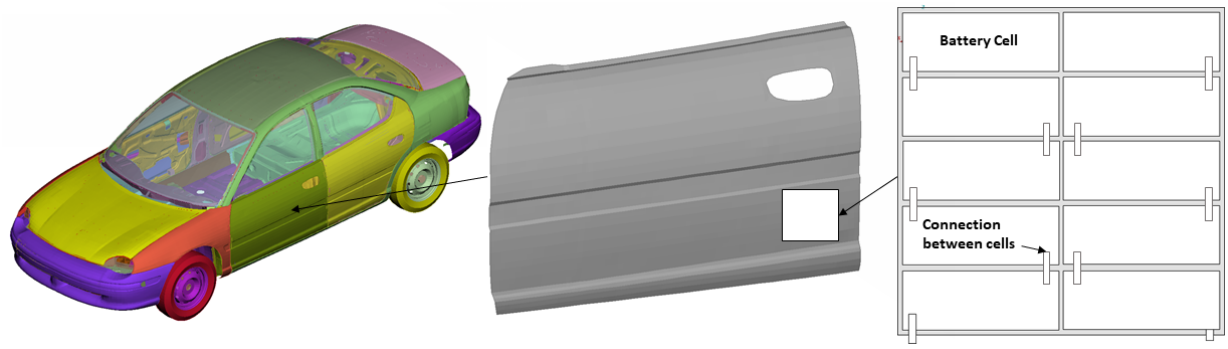

Structural Battery Composites in Electric Vehicle Design

A Feasibility study

Master's thesis in Applied Mechanics

Rishab Rangarajan

Department of Industrial and Materials Science
CHALMERS UNIVERSITY OF TECHNOLOGY
Gothenburg, Sweden 2018

Master's thesis 2018:06

Structural Battery Composites in Electric Vehicle Design

Master Thesis Report

Rishab Rangarajan

CHALMERS
UNIVERSITY OF TECHNOLOGY

Department of Industrial and Materials Science
Division of Material and Computational Mechanics
Chalmers University of Technology
Gothenburg, Sweden 2018

Structural Battery Composites in Electric Vehicle Design
Master Thesis Report
Rishab Rangarajan

Supervisor: David Carlstedt, Department of Industrial and Materials Science
Examiner: Leif Asp, Department of Industrial and Materials Science

Master's Thesis 2018:06
Department of Industrial and Materials Science
Division of Material and Computational Mechanics
Chalmers University of Technology
SE-412 96 Gothenburg
Telephone +46 31 772 1000

Cover: Structural battery composite setup in a vehicle's structural component

Typeset in LaTeX
Printed by [Name of printing company]
Gothenburg, Sweden 2018

Structural Battery Composites in Electric Vehicle Design
Rishab Rangarajan
Department of Industrial and Materials Science
Division of Material and Computational Mechanics
Chalmers University of Technology

Abstract

Multi-functional materials is the new venture for the automotive industry in terms of light-weighting. However, due to the infancy of this technology the adoption of these materials still has to be evaluated. A holistic design must be adopted to effectively utilise the multi-functional capabilities of the material unlike current design methodologies. Currently, the structural and electrical requirements for an electric vehicle are outlined and evaluated individually. In this research, a framework for evaluating the feasibility on a holistic level is built. The feasibility is based on the total driving range of the vehicle as well as the ability to contribute to the structural integrity of a vehicle.

Keywords:Carbon fibre reinforced plastics, Multifunctional materials, Structural battery composites, Energy storage, Structural efficiency, Electrical efficiency

Acknowledgements

I would like to take the opportunity to thank Chalmers University of technology to provide the platform for the research done. The work done would not have been possible without the constant support of my supervisor, David Carlstedt. I owe Leif Asp for pushing me past my limits and making sure i provide valid as well as revolutionary results. The constant support from my friends for all the night long work put into completing the research is also of great importance to me.

Rishab Rangarajan, Gothenburg, July 2018

Contents

List of Figures

List of Tables

1

Introduction

Industrialisation and urbanisation are key drivers for the automotive market. Due to the increasing demand for transportation and the increased awareness of the environmental impact of current technical solutions, there is an increasing concern on emission levels and carbon footprint. Various strategies are currently being explored to meet future requirements on environmental impact including alternative fuels, lighter materials, more efficient vehicles, etc. Two of the most implemented strategies are electric vehicles and using lighter materials. By reducing the weight of the structural architecture of the vehicle by using lighter material, it is possible to further downsize the vehicle components, motors, transmission components, etc. following the light-weighting spiral illustrated in Figure 1.1

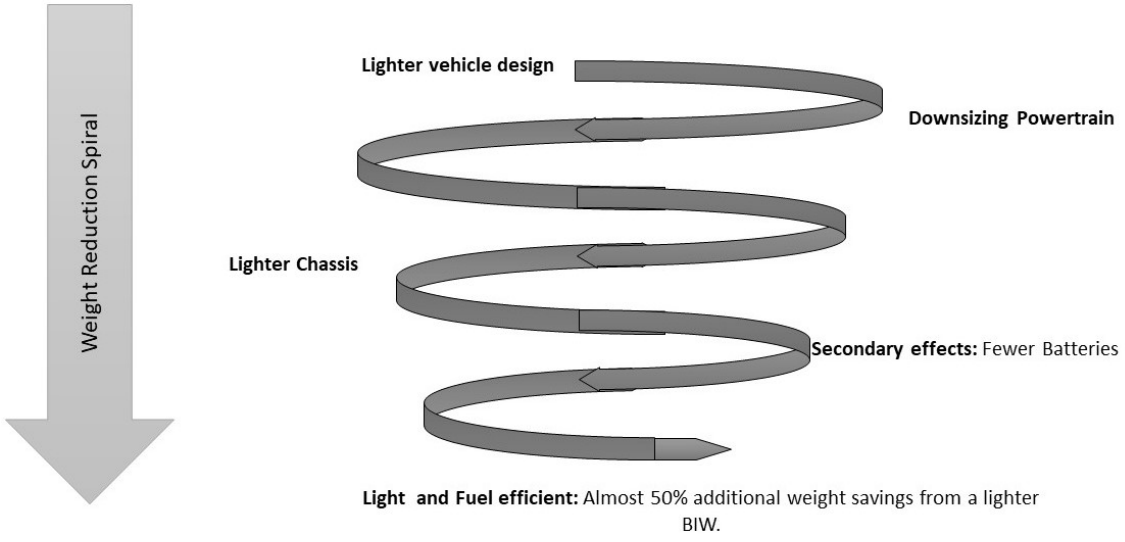

Figure 1.1: Lightweighting spiral for electric vehicles

The potential weight savings are evident in Figure 1.1. Multi-functional materials is a viable option to gain further momentum on this front. As the name suggests these materials perform more than a one function. One such category is the structural power composites. These materials provide structural as well as electrical performance. Incorporating these materials in an electric vehicle offers the possibility to significantly reduce the total weight of the vehicle due to the added functionality

of mass less energy storage. Especially when incorporated into the Body-in-white (BIW) of vehicles.

The structural power composites can be considered equivalent to batteries or capacitors. There are various types of structural power composites based on the funtionality of the constituents and the architecture of the composite. The research in this study focuses only on structural battery composites.

Following the work done by Scholz [1] and Asp and Greenhalgh [2] the current study evaluates the feasibility and potential benefits in incorporating structural battery composites in electric vehicles. In this study this material is perceived to be incorporated within various components in the structural architecture of the vehicle.

By predicting the weight of the vehicle and the perceived battery capacity the total vehicle range can be estimated. This gives an insight into adopting a holistic vehicle design with a constraint on the total vehicle weight as well as the amount of structural battery composite required to meet a required range. The following structural analysis gives an overall picture of the structural properties of the vehicle, the battery distribution and the potential weight savings.

1.1 Structural power composites

This chapter gives a brief overview of the architecture of structural battery composites as discussed by Asp and Greenhalgh [2]. Carbon fibre reinforced polymer (CFRP) composites are mainly used in structural battery composites due to the high mechanical and electrical capacities of the carbon fibres [3]. For the matrix in the structural battery composite, a bi-continous polymer system is often used where a liquid electrolyte is combined with a thermoset porous matrix [4]. This combined solid and liquid polymer matrix is used to provide high structural and electrical performance. The concept of replacing battery constituents with structural components in structural battery composites is illustrated in Figure 1.2.

There are two concept designs for the structural battery composite, namely:

- 3D design
- 2-D laminate design

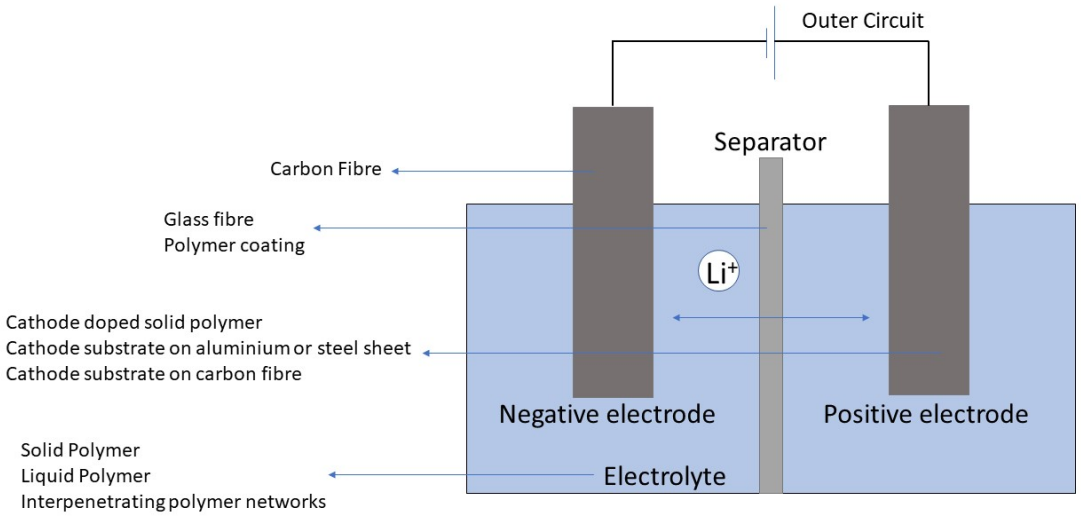

Figure 1.2: Illustration of the concept of replacing battery constituents with structural components in structural battery composites [5]

1.1.1 3-D battery design

The 3-D structural battery composite was developed by Asp and co-workers [6, 7, 8, 9]. In the 3D design, the fibres act as negative electrodes in the battery cell. Each of these fibres are coated with a thin polymer coating acting as a combined electrolyte and separator layer. The surrounding polymer matrix is doped with positive electrode materials (eg. $LiFePO_4$) which acts as the positive electrode in the battery cell. The setup of a typical 3-D battery is depicted in Figure 1.3.

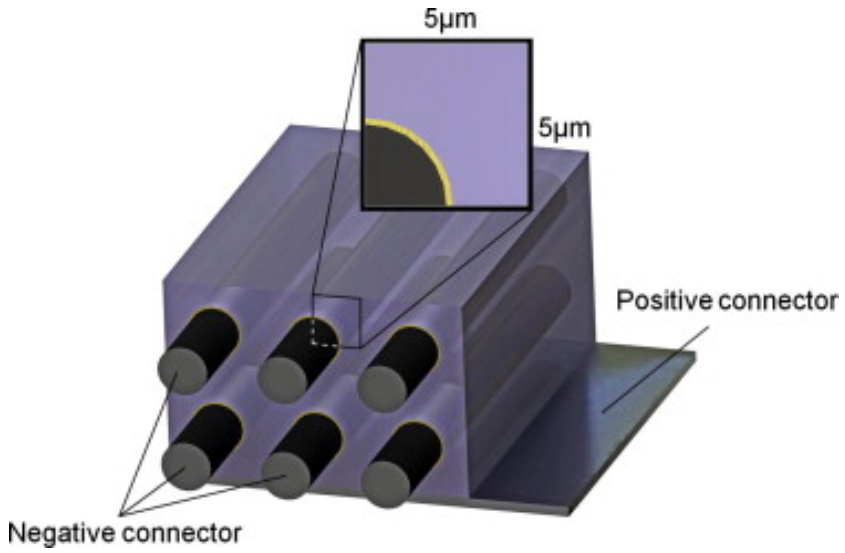

Figure 1.3: Schematic illustration of the 3-D structural battery composite [2]

The analysis in this study is performed only for 2-D laminate design which is discussed in the following section.

1.1.2 2-D Laminate battery design

The 2-D laminated battery concept was first proposed by Wetzel et.al [10, 11] and later demonstrated by Ekstedt et al. [12] and Carlstedt et al. [13]. In this architecture each laminae has a separate function in the battery cell and works as an electrode, separator, reinforcement, etc. The active materials in the negative electrode lamina in the carbon fibres. The fibres in the lamina which acts as the positive electrode is coated with a binder containing positive electrode material, generally lithium metal oxide (eg.$LiFePO_4$). The coating also contains carbon black particles to increase conductivity. The separator is added to prevent the electrode to come in contact and the reinforcement plies are added for protection and increases the mechanical performance. The packaging material prevents any moisture from diffusing into the battery. This is depicted in Figure 1.4.

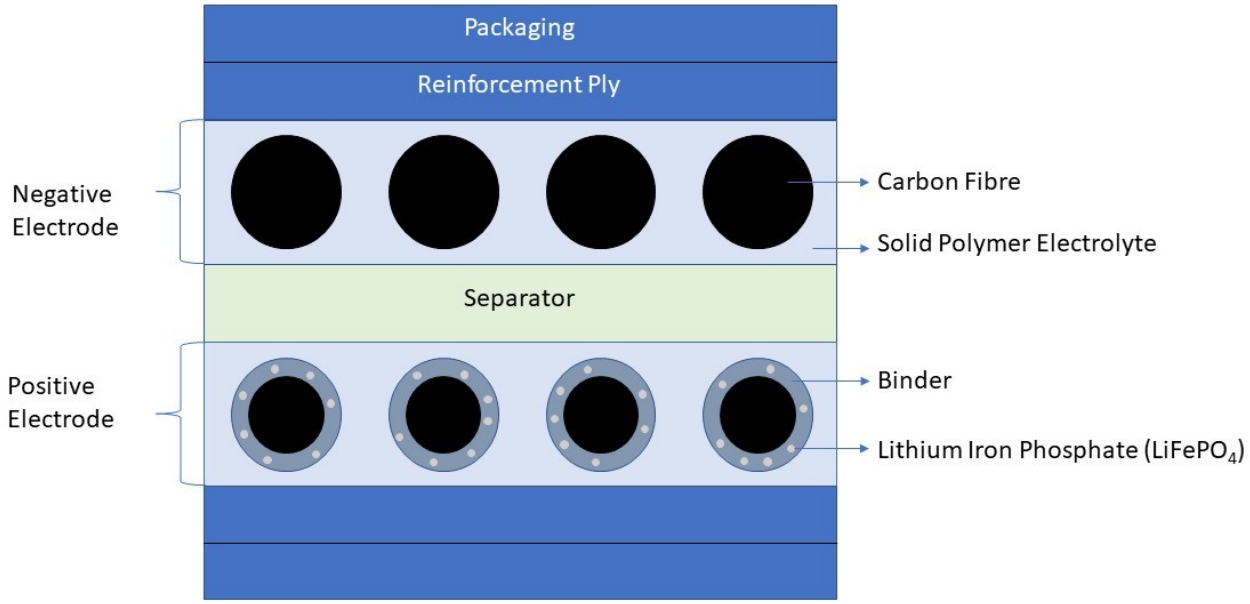

Figure 1.4: 2-D laminate layout cross sectional view

1.2 Multi-functional performance

The metrics to determine the performance of multi-functional materials have to be based on the multiple properties built into the material. For structural battery composites it has to be a combination of the load bearing capabilities as well as the battery capacity to store electrical energy. As discussed by O'Brien et. al. [14], to measure the performance or maturity of a multi-functional material, one would have to consider the mass of the total system, the electrical efficiency and the

structural efficiency. This is crucial to develop a sound methodology for evaluating the feasibility of using structural battery composites in electric vehicles.

1.3 Aim and approach

The aim of the study is to evaluate the feasibility and potential benefits of adopting structural battery composites in electrical vehicles. To benchmark the performance, a predictive range model is developed to estimate the range of an electric vehicle using traditional mono-functional batteries. Then, the range of the same vehicle is estimated when the existing mono-functional batteries are replace with component made of structural battery composites. By matching the total range of the benchmark the needed mass of structural battery composite can be estimated. Following this, a structural analysis is performed for a structural component within the vehicle to determine the structural efficiency of the material.Finally the feasibility of replacing existing vehicle components with components made out of structural battery composites is discussed and potential weight savings are estimated.

1.4 Limitations and scope

The electric performance is based on the energy storage capabilities and not the power delivering capability. Additionally, the internal resistance, discharge characteristics and the Peukert's coefficient are assumed to be similar to that of Li-ion batteries.

The structural performance is evaluated on a component level rather than for the whole vehicle. The structural performance is evaluated only for oil canning and no other loading case.

While there is a need for a holistic vehicle design to effectively utilise structural battery composite, the research conducted is based on substituting the materials in existing components with structural battery composites.

This study does not look at feasibility from a manufacturing perspective.

2

Theory

The multi-functional nature of the material requires high interdependence between the properties in concern. This chapter discusses the background theory used in thr current study.

The theory discussed draws parallel to the fundamental principles required to analyse the electrical performance as well as the structural performance. For the electrical performance, we discuss the requirements from the vehicle and simulate it in real world situations using a standardised drive cycle. The structural performance depends on the component studied along with the appropriate elastic characteristic required. Finally, the interaction between the individual performance is linked to determine the maturity of the structural battery composite presented.

2.1 Range modelling

The range that is predicted is the total distance the vehicle can drive given a total battery capacity. The range predicted is based on the range model (including the battery model) and assumed drive cycle. In this the 'New European Drive Cycle' (NEDC) is used. The drive cycle simulate typical driving characteristics or usage of a vehicle in Europe.

Based on the drive cycle the tractional power, the depth of discharge (DOD) and the corresponding distance travelled is calculated.

2.1.1 NEDC drive cycle

The NEDC cycle can be divided into two main parts. The first being the Urban drive cycle or 'UDC' ($0 - 1500$ *steps*) and the second being the Extra-Urban drive cycle ($1500 - 2300$) depicted in Figure 2.1. The UDC phase simulates typical driving conditions in European cites. The Extra urban phase simulates a more aggressive driving style with high speed driving. The overall distance travelled in one drive cycle is approximately 10 km in a total of 1180 s with the maximum speed in both phases being 50 and 120 km/h respectively.

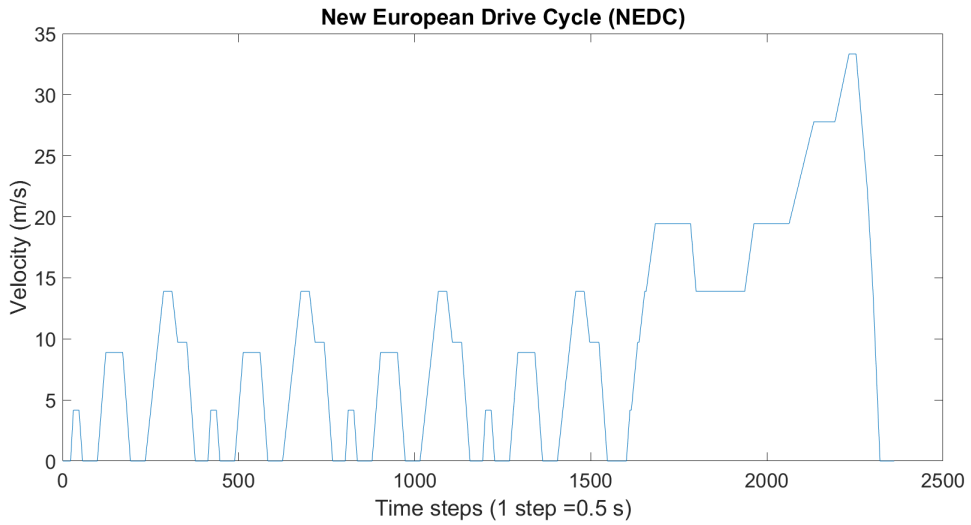

Figure 2.1: NEDC cycle with velocity on the Y-axis and number of time steps (1 step=0.5 s) on the X-axis.

2.1.2 Tractional power

Based on the driving cycle, one can calculate the acceleration of the vehicle. Given the acceleration and mass of a vehicle, the tractional force (F_{te}) can be calculated. The tractional force is the force applied on the vehicle to accelerate over the given period of time. This is based on the aerodynamic drag (F_{ad}), hill climbing force (F_{hc}), rolling resistance (F_{rr}), the force required for linear acceleration (F_{la}) and angular acceleration ($F_{\omega a}$).

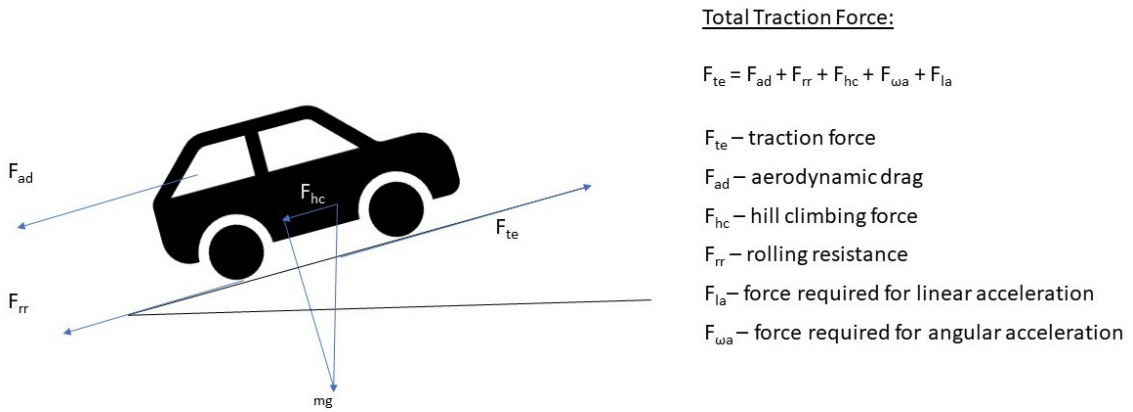

Figure 2.2: Tractional force in a moving vehicle

The aerodynamic drag is based on the coefficient of drag of the vehicle (C_d) and the frontal area. The hill climbing force is zero as for the the NEDC cycle, as the vehicle is assumed to travel on a flat surface. The rolling resistance is based on the mass of the vehicle and the coefficient of friction or rolling resistance (C_{rr}). To account for the angular acceleration, a mass factor (F_m) is introduced [16]. Based on the

velocity, the vehicle will be accelerating or decelerating. Hence the tractional force, while decelerating will be the braking force. This force gives the velocity and the corresponding tractional power (P_{te}). This is the power delivered to the wheels by the transmission. This is elaborated in Equations 2.1-2.5.

The aerodynamic drag force is defined as:

$$F_{ad} = \frac{1}{2} \cdot \rho \cdot A_{front} \cdot C_d \times (V - V_w), \tag{2.1}$$

where, ρ is the density of air, A_{front} is the frontal area, V the vehicle velocity of the vehicle and V_w is the wind velocity (= 0 for NEDC cycle).

The rolling resistance is defined as:

$$F_{rr} = M \cdot g \cdot C_{rr} \cos\theta, \tag{2.2}$$

where, M is the mass of the vehicle and g is the acceleration due to gravity and θ the angle of inclination (= 0 for NEDC cycle). The total force due to acceleration is defined as:

$$F_{la} + F_{\omega a} = F_m \times M \cdot Acc, \tag{2.3}$$

where Acc is the acceleration. Finally, the traction power are defined as:

$$F_{te} = F_{ad} + F_{rr} + F_{hc} + F_{\omega a} + F_{la} \tag{2.4}$$

$$, P_{te} = F_{te} \times V, \tag{2.5}$$

2.2 Electrical performance

The electrical performance is crucial for determining the feasibility of the structural battery composite. It is based on the mechanical power required to drive the vehicle. This mechanical requirement is translated to the electrical energy that has to be provided by the battery. This is then linked to the battery capacity and the mass of the battery. There are various factors that need to be considered to determine the total capacity of the structural battery composite and how this capacity changes as the vehicle progresses in the NEDC cycle.

2.2.1 Nominal capacity and specific capacity

The specific capacity (Ah/kg) of a battery links the total nominal capacity to its weight. The battery capacity is calculated for one cell and depending on the battery arrangement the total capacity of the battery pack is determined.

The battery capacity was calculated as in Equation 2.6

$$Capacity = N_{cell} \times (W_{cell} \times \mu_{cell}) \tag{2.6}$$

Where N_{cell} is the number of cells.

2.2.2 Peukert's law

While the nominal battery capacity indicates the total energy stored in the battery, the total usable energy is not the same. This depends on the discharge rate of the battery. For this purpose, the Peukert's law determines the actual capacity of the battery based on the discharge rate. The relation based on the law is defined as:

$$C_p = (I^k) \times T \tag{2.7}$$

$$, I = \frac{Capacity}{T}, \tag{2.8}$$

In Equations 2.7 and 2.8 C_p is the Peukert Capacity, T the time for discharge and k the Peukert coefficient. The Peukert coefficient is specific to battery type. In general, for Li-ion batteries it is taken as 1 due to the inherent nature of the battery to heat up during rapid discharge. However, in the research by Omar et. al. [15] it varies between $1 - 1.1$.

2.2.3 DOD vs Open circuit voltage

The open circuit voltage (E) depends to a high degree on the DOD. The discharge characteristic of a battery depends on the type of battery [16]. The DOD varies from $0-0.9$ where 0 corresponds to a completely charged battery and 0.9 to a battery that is 90% discharged. No battery is ever completely discharged especially in automotive usage. Based on the depth of discharge the open circuit voltage changes. the open circuit voltage of the structural battery composite battery cell is assumed to be

$$E = N_{ser} \times (4 - DOD \times (4 - 3)) \tag{2.9}$$

Here it is seen that the open circuit voltage (E) varies from 4 to 3 as the depth of discharge varies from 0 to 1. In Equation **??**, N_{ser} is the number of cells connected in series. This dependency varies for different types of batteries.

The typical discharge characteristics for a Li-ion battery used in automotive vehicles in this research was based on the work done by Omar et al. [15]. The typical discharge characteristics for a Li-ion battery varying from 3.7 to 2 for varying rate of discharge and is depicted in Figure 2.3. This is the characteristics for a battery with high energy capabilities.

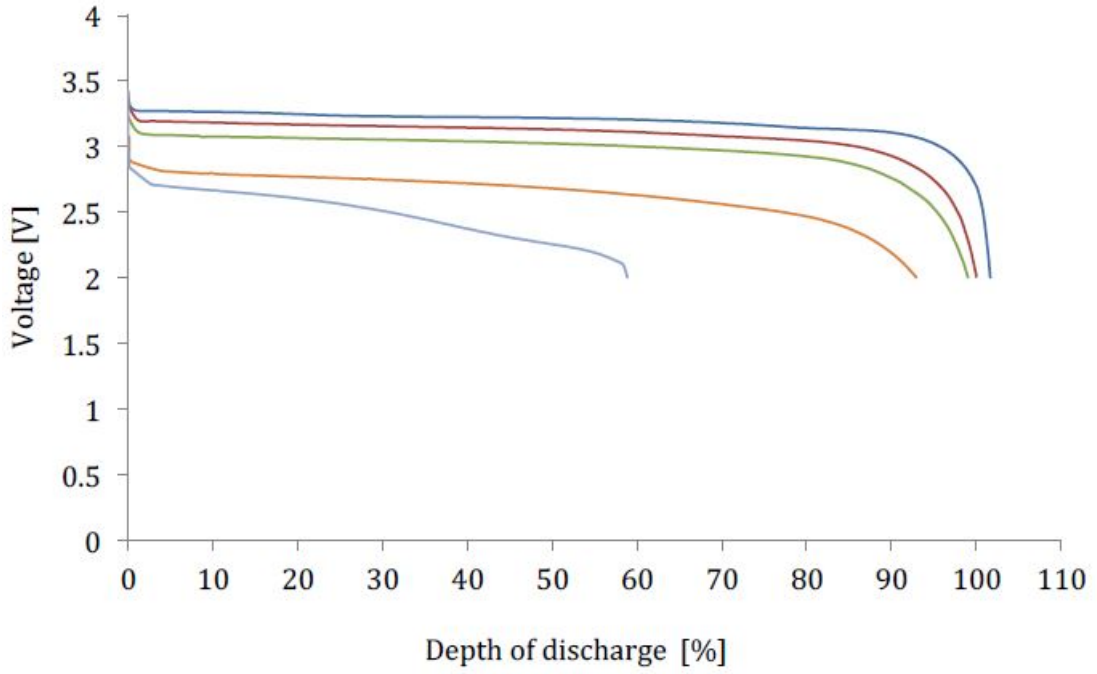

Figure 2.3: Discharge characteristics for high energy Li-ion batteries [15]

2.2.4 Charge removed and DOD

The charge removed from the battery is determined by the current provided to drive the motor of the vehicle. The current (I) depends on the power provided by the battery (P_{bat}), the internal resistance of the battery (R_{int}) and the open circuit voltage (E). From the mechanical power, the power that needs to be provided by the battery can be determined. This power is determined as:

$$P_{bat} = V \times I = (E - I \times R_{int}) \times I \rightarrow P_{bat} = E \times I - R_{int} \times I^2. \tag{2.10}$$

To meet the power requirements from the motor the power delivered by the battery needs to be equal to the power required to move the vehicle.

$$P_{bat} = P_{te} \tag{2.11}$$

On rearranging and solving the quadratic equation 2.10, the current provided by the battery can be determined as:

$$I = \frac{E \pm \sqrt{E^2 - 4 \times R_{int} \times P_{te}}}{2 \times R_{int}}. \tag{2.12}$$

In the case of $E^2 - 4 \times R_{int} \times P_{te} \leq 0$, the battery pack is not able to provide the power required for the vehicle. Based on the current from Equation 2.12, the charge removed (CR) from the battery (for the given change in velocity) and hence the

depth of discharge (DOD) can be calculated as depicted in equations 2.13 and 2.14

$$CR = \frac{\delta t \times I^k}{3600} \tag{2.13}$$

$$, DOD = \frac{CR}{C_p}. \tag{2.14}$$

In Equation 2.13 and 2.14, CR is the charge removed for the given current delivered by the battery and δt is the time in which the current is provided. The corresponding depth of discharge DOD is based on the charge removed from the peukert capacity C_p [16].

As explained the DOD is the extent to which the battery has been discharge, hence it is evident that the ratio of the charge removed to the total working capacity will determine the depth of discharge. When the analysis is performed, this is a cumulative process. Hence the total charge removed is a summation from previous time-steps.

2.3 Structural performance

The structural performance of the composite is assessed by estimating the stiffness determined based on classical laminate theory (CLT). The composite layup is assumed to consist of uni-direction laminae stacked on top of each other. The elastic properties of the individual lamina are determined using the micro-mechanical model's rule of mixtures (ROM) and Halpin-Tsai model [17].

The longitudinal Young's modulus (E_{11}) and the major Poisson's ratio (ν_{12}) is determined by ROM while the transversal Young's modulus (E_{22}) and the longitudinal shear modulus (G_{12}) is defined as:

$$E_{11} = V^f \cdot E_{11}^f + V^m \cdot E^m \tag{2.15}$$

$$, \nu_{12} = V^f \cdot \nu_{12}^f + V^m \cdot \nu^m \tag{2.16}$$

$$, E_{22} = E^m \cdot \left(\frac{1 + \zeta \eta V_f}{1 - \zeta \eta V_f} \right) \tag{2.17}$$

$$G_{12} = G^m \cdot \left(\frac{1 + \zeta \eta V_f}{1 - \zeta \eta V_f} \right) \tag{2.18}$$

$$, with\ \eta = \left(\frac{\frac{M_f}{M_m} - 1}{\frac{M_f}{M_m} + \zeta} \right), \tag{2.19}$$

with $\zeta = 1$ and 2, and $M = E\ or\ G$ for E_{22} and G_{12} respectively.

In Equations 2.15 - 2.19, V^f and V^m are the volume fractions of the fibres and matrix respectively. Similarly, E^m, ν^m and G^m are the Young's modulus, Poisson's ratio and Shear modulus of the matrix. The factor ζ is a factor that depends on the fibre geometry.

While the micro-mechanics is determined, the macro-mechanics of the structural battery composite is determined using the classical laminate theory. Following the CLT, the stiffness matrix Q is dependant on the thickness and orientation of each lamina. For the laminate we have uniform and unidirectional laminae. Following CLT the stiffness matrix is defined in Equation 2.20, assuming transverse isotropy and plane stress

$$Q = \begin{bmatrix} \frac{E_{11}}{1-\nu_{12}\nu_{21}} & \frac{\nu_{12}E_{22}}{1-\nu_{12}\nu_{21}} & 0 \\ \frac{\nu_{21}E_{11}}{1-\nu_{12}\nu_{21}} & \frac{E_{22}}{1-\nu_{12}\nu_{21}} & 0 \\ 0 & 0 & G_{12} \end{bmatrix} \tag{2.20}$$

$$A_{ij} = \sum_{k=1}^{n} \left[(\overline{Q_{ij}})\right]_k (h_k - h_{k-1}) \qquad i = 1,2,6; \quad j = 1,2,6 \tag{2.21}$$

$$B_{ij} = \frac{1}{2} \sum_{k=1}^{n} \left[(\overline{Q_{ij}})\right]_k (h_k^2 - h_{k-1}^2) \quad i = 1,2,6; \quad j = 1,2,6 \tag{2.22}$$

$$D_{ij} = \frac{1}{3} \sum_{k=1}^{n} \left[(\overline{Q_{ij}})\right]_k (h_k^3 - h_{k-1}^3) \quad i = 1,2,6; \quad j = 1,2,6 \tag{2.23}$$

From Equations 2.21-2.23 the A, B and D components depend on the stiffness matrix defined with the directional properties of the individual lamina in the co-ordinate system of the laminate ($\overline{Q} = T_6^{-1} Q \cdot T_\xi)\overline{Q}$ and the thickness of the laminae . In the case of a balanced and symmetric laminate B and D components, gives zero. Hence only the A matrix exists. This is how the mechanical properties of the structural battery composite is determined.

2.4 Multi-functional performance

The total mass reduction according to O'Brien's model states that:

$$M - M^* = (1 - \eta^e - \eta_i^s) \times m_{sbc} \quad \text{Where } \eta^e + \eta_i^s > 1 \tag{2.24}$$

Where η^e is the electrical efficiency and η_i^s is the summation of the structural efficiency of each individual structural component. The efficiencies as mentioned in the previous section depend on the vehicle range, mass of the vehicle, total capacity and mass saved. The electrical efficiency is linked to the energy used vs. the energy available originally. The Equation 2.25 determines the electrical efficiency.

$$\eta^e = \frac{\frac{R_{sbc} \cdot M^*}{C_{sbc}}}{\frac{R_{bat} \cdot M}{C_{bat}}} \tag{2.25}$$

Where R_{sbc} and R_{bat} are the driving range using the corresponding power source while, C_{sbc} and C_{bat} are the battery capacities.

To determine the exact maturity of the material, from a structural perspective, we determine how much of the material is utilised in the structural architecture of the vehicle. There will be cases where the total structural battery composite will be substituted in the components as well as vice versa where we might not have enough structural battery composite available. Hence, it is important to evaluate the structural efficiency based on usage. This utilitarian efficiency (Equation 2.26) will depict the multi-functional utility of the structural battery composite.

$$\eta^s = \sum_{i=1}^{n} \frac{m_i - m_i^*}{m_{sbc}} \tag{2.26}$$

Hence the total multi-functional performance is the sum of the electrical and the structural performance defined as seen in Equation 2.27.

$$\eta = \eta^e + \eta^s \tag{2.27}$$

This sum of the efficiencies should be greater than one for the maturity of the structural battery composite as given by the O'Brien's Model.

3

Methodology

The range is predicted using MATLAB. The algorithm and code was compiled based on the available code developed by Larmine and Lowry [16]. The model calculates the total range of the vehicle based on assumptions regarding the vehicle mass, battery characteristics, drive cycle, etc.

3.1 Procedure

The predictive model is initially configured for the given vehicle using mono-functional batteries. This helps fixing the parameters specific to the vehicle, namely total depth of discharge, the power to auxiliary systems, the regenerative ratio, etc. Once the range is predicted, the configured model with the same parameters is used to predict the range for the revised mass of the vehicle and the total capacity on substituting with structural battery composite. This process is repeated for the various case studies.

3.2 Algorithm

The predictive model runs a nested loop where the distance travelled is calculated for every step of the NEDC cycle. This is repeated until the maximum allowed depth of discharge is reached as depicted in Figure 3.1 (in this study, the maximum DOD is 0.9). To do this, the data of the drive cycle is loaded and the assumed parameters for the vehicle and battery are given as inputs specific for a given model. Following this, the nested loop runs calculating the tractional power and hence the battery power. When calculating the battery power, the corresponding current required is determined. Based on the current, the charge removed for the current time step is added to the sum total of charge removed from previous time steps giving the total charge removed. Finally, this translates to the depth of discharge. If the battery has not reached the maximum allowed depth of discharge the distance travelled is calculated and the procedure inside the nested loop is repeated for the next velocity cycle.

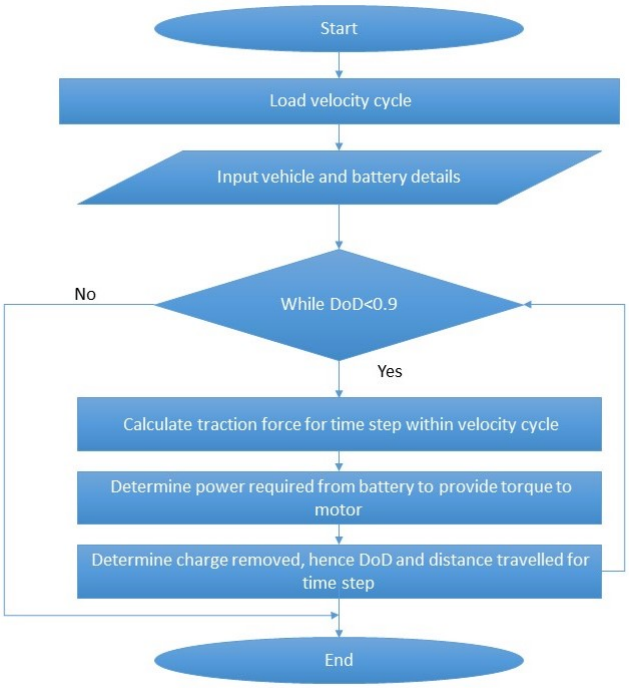

Figure 3.1: MATLAB algorithm to calculate electric vehicle range [16]

3.3 Range analysis- case studies

Range analysis is done for two cars on either end of the spectrum namely, Tesla Model S (total energy 75 kWh and total mass 2100 kg) and the BMW i3 (total energy 33 kWh and total mass 1300 kg). These two cars have a range around 500 km and 300 km respectively. Comparing the vehicle range and the battery capacity, there is a stark difference and this is mainly linked to the mass of the vehicles. They both have very good light-weighting strategies. The Tesla Model S has an Aluminium "space frame" and the BMW i3 has a Carbon fibre composite "life module". It is for these reasons that we believe that the two cars are assumed to be on either end of the spectrum and are viable for study in terms of a feasibility study.

Each vehicle has three case studies each. These cases studies are used for determining the driving range of the vehicle using different amounts of structural battery composite. The logic for the case studies are as listed below.

- Case 1
  - Remove existing mono-functional battery
  - Introduce structural battery composite within the vehicle structure based on realistic assumptions
- Case 2
  - Double the thickness of the structural battery composite as present in

Case 1

- Case 3
  - Remove existing battery and identify the amount of structural battery composite required to meet the existing vehicle range.

Building a realistic model as in case 1 and 2 will require a few parameters to be considered. There are constraints on the space available as the density of the existing battery and the composite vary by a factor of 2-3 depending on the material. As a conventional battery is packaged compactly, a structural battery composite of lower density would require more space for packaging. The third case will depict the feasibility of using structural battery composite to meet the same vehicle performance. The crumple or crash zones of the vehicle are not considered suitable for substitution at this point due to its unpredictable nature of composites in such impact situations.

3.3.1 Tesla Model S

The breakdown of the weight within each system of the Tesla Model S is presented in Table 3.1. Based on this, structural battery composites are introduced in the space frame, the interior trims and the exterior panels of the vehicle. For all the cases, the existing Li-ion battery is removed.

Vehicle system	**Weight of system (kg)**
Battery	600
Aluminium space frame	365
Motor and drive train	465
Electrical	100
Interior	300
Exterior	90
Miscellaneous	180
Total	**2100**

Table 3.1: Tesla Model S weight analysis [21]

To build the case studies, the total weight of the existing battery is removed. For Case 1, around 40 percent of the space frame is substituted with structural battery composite and not the whole space frame to avoid crash zones present in the front and back of the vehicle, constraining ourselves to the passenger cabin. Additionally, around 80 percent of the interior and exterior panels are substituted with structural battery composites. The stiffness of the interior and exterior panels are often provided by the geometry added underneath. Hence, when replacing the existing

interior panels the structural battery composite can be introduced as illustrated in Figure 3.2.

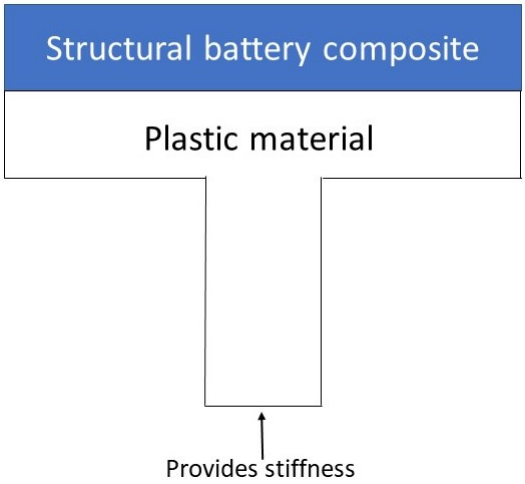

Figure 3.2: Illustration of potential solution for replacing parts of interior panels with structural battery composite. Back injected plastic added to provide stiffness

This means that most of the interior and exterior panels can be replaced with structural battery composite but 20% is kept as is due to geometric limitations, connection points, etc.

As explained earlier for case 2, the thickness of the structural battery composite used is doubled, hence the mass of the structural battery composite is doubled. This might not be an optimal solution from a weight saving perspective but would be a viable option to implement due to the limited need for modification and packaging.

For case 3, the amount of structural battery required (W_{sbc}) is estimated without increasing the vehicle weight while removing the battery and meeting the range predicted for the existing vehicle. The required battery capacity (C_{sbc}) can be estimated roughly by maintaining the ratio of the original battery capacity to the original weight of the vehicle. The summary of the 3 cases are as listed in Table 3.2.

Case study	**Car weight (kg)**	**Composite weight (kg)**	**Total capacity (Ah)**
1	1500	300	75
2	1800	600	150
3	1500	W_{sbc}	C_{sbc}

Table 3.2: Case studies analysed for Tesla Model S

The battery characteristics used in the predictive model for the original Tesla Model S are as listed below in Table 3.3.

Parameter	Value
Total energy	85 kWh
Total capacity	210 Ah
Auxiliary power	100 W

Table 3.3: Specifications of battery in original Tesla Model S

3.3.2 BMW i3

The weight of the BMW i3 is estimated based on a comparative analysis with the Model S. The estimation is validated for the weight of vehicle systems available from online sources [23, 24]. The estimation is also further adjusted based on the total weight of the vehicle and based on the material composition of the vehicle. The weight analysis for the BMW i3 is presented in Table 3.4.

Vehicle system	Weight of system (kg)
Battery	230 [23]
Life module	140 [24]
Drive module	480
Electrical	80
Interior	188
Exterior	57
Miscellaneous	140
Total	**1300**

Table 3.4: BMW i3 weight analysis

Similar to the Tesla Model S, case studies are built to analyse the vehicle with structural battery composite. Due to the existing use of fibre reinforced polymer within the vehicle, around 80 percent of the mass of the life module is assumed to be substituted with structural battery composite. Additionally, 50 percent of the interior and exterior panels are substituted with structural battery composite. For the second case study, the thickness of the structural battery composite is doubled as for the Tesla. Similarly, the third case is also developed as mentioned in the previous section to determine the weight and structural battery capacity (W_{sbc}, C_{sbc}). A summary of the case studies are listed in Table 3.5.

Case study	Car Weight (kg)	Composite Weight (kg)	Total Capacity (Ah)
1	1070	150	8
2	1230	300	15
3	1070	W_{sbc}	C_{sbc}

Table 3.5: Case studies analysed for BMW i3

The battery characteristics used in predictive model for the original BMW i3 are listed in Table 3.6.

Parameter	Value
Total Energy	33 kWh
Total Capacity	90 Ah
Auxiliary Power	200 W

Table 3.6: Specifications of battery in BMW i3

3.4 Structural battery application in electric vehicles

In the research performed, The specific capacity of the structural battery composite is assumed to be 25 Ah/kg (μ_{cell}) and the weight of one cell (W_{cell}) is assumed to be 0.04 gm. These assumptions are based on assuming individual battery battery cells with the dimensions of $15x15x0.1$ cm and cell properties derived using the framework developed by Carlstedt et al [19]. These properties are summarised in Table 3.7. In order to meet the requirements of an electric vehicle , 100 structural battery cells are arranged in series to get 400 V assuming a nominal voltage discharge of $4V$. The rest of the battery cells are distributed in parallel to maximise the current possible to extract. The NEDC is used as our velocity cycle.

For the research done in this study, the Peukert coefficient is assumed to be 1.1 for both the Li-ion batteries as well as the structural battery composite. The time for discharge (T) in both cases is 1 hour.

Parameter	Value
Mass of one unit cell	0.040 kg
Dimension of one cell	15 ×15 ×0.1 cm
Specific Capacity	25 Ah/hg
Specific Energy	0.1 kWh/kg
Internal Resistance	0.02 Ω [15]
Peukert Coefficient	1.1 [15]
Time for discharge	1 Hour
Velocity Cycle	NEDC
Depth of Discharge	0.9

Table 3.7: Assumed battery properties based on ordinary Li-ion batteries and framework used in the predictive model in MATLAB

The internal resistance of the battery (R_{int}) is the effective resistance based on the number of cells connected in series and parallel. Given the internal resistance of one cell is (R), the number cells in series (N_{ser}) and those in parallel (N_{par}) the effective internal resistance is calculated:

$$R_{int} = \frac{N_{ser} \times R}{N_{par}} \tag{3.1}$$

One unit of the structural battery composite is assumed to consists of 10 cells connected in series as seen in Figure 3.3. Connecting 10 such units in seriers and assuming a nominal voltage of 4 V per cell, gives a total voltage of 400 V. The remaining units are stacked or placed such that series units are connected in parallel. Hence the total battery capacity is determined by Equation 2.6.

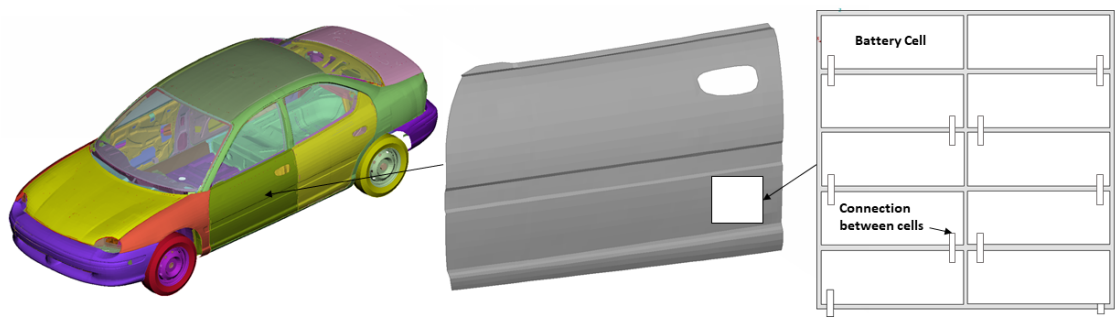

Figure 3.3: Illustration of the battery setup in one component in a FE model of a car [18]. One unit containing 10 battery cells connected in series.

3.4.1 Stiffness vs strength

With respect to the mechanical performance of the structural battery composite, only the stiffness of the material is considered. Hence, the physical failure is not evaluated. The stiffness of the composite will help in determining its ability to resist deformation. The phenomenon of oil canning is the ability of the panel to resist permanent deformation on applying force by just a hand or leaning against the door. The metric for measuring the structural performance would be the ability to resist this deformation hence the flexural stiffness is the most ideal in terms of the performance model.

3.4.2 FE analysis

To evaluate the structural performance of a component made out of structural battery composite. A generic FE model of a car was taken from the Altair Database [18]. The model is then loaded on ANSYS and the door panel was isolated by hiding the other components. The original material (steel) properties was maintained for the first analysis to be the bench marking performance. The constrains and loading were set to simulate oil canning loading. The panel was then substituted with the composite material, and the material properties used were the elastic properties calculated in MATLAB based on the framework from [19].

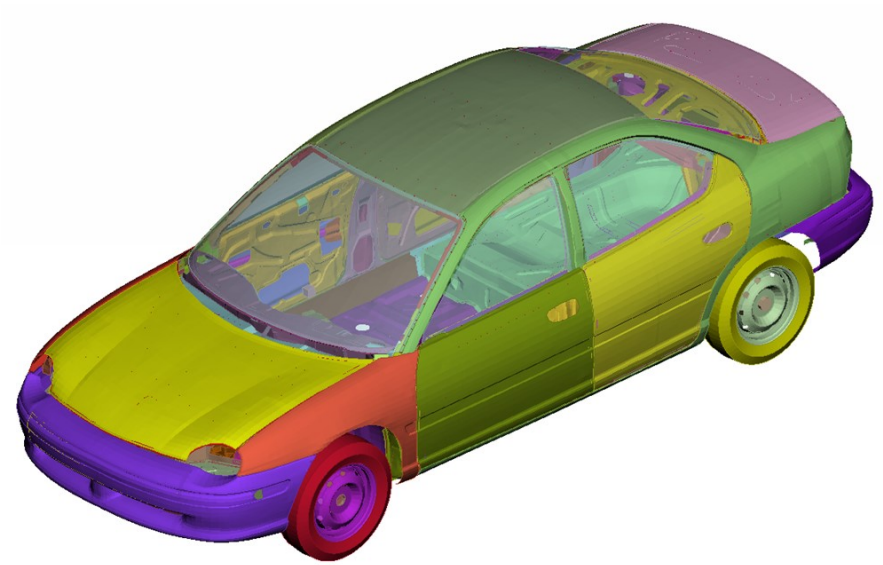

Figure 3.4: FE model of a car obtained from Altair database [18]

4

Results and discussion

In this section the results obtained and its relation to the multi-functional performance model explained in the Section 2.4 is discussed. The analysis is a comparative analysis to determine the feasibility of the structural battery composite. The bench marking analysis is done using the metrics specified in the modified O'Brien's model.

4.1 Range model

The range analysis is performed using the predictive range model described in Section 3.2. The analysis is first done for case 1 and 2 which will then help in determining the weight of structural battery composite (W_{sbc}) required in the third case. The metrics important for bench marking and feasibility are

- Mass of vehicle
- Total battery capacity
- Weight of structural battery composite
- Total vehicle range

The analysis was done for both the Tesla Model S and BMW i3 as mentioned earlier.

4.1.1 Tesla Model S

The predicted range capacity and mass for the three cases described in Section 3.3 for the Tesla Model S with the structural battery composite as well as the original battery range of the configurations are depicted in Figure 4.1. To benchmark with the other vehicles, the original Tesla is predicted using the range model. The range of the original vehicle is estimated to be around 320 km. This is less than the rated range.This could be due to the lack of detail available to public and the simplicity of the model built. For case 1 the total driving range is around 150 km. While this is less than the the original case, on comparing with the rated NEDC range, around $50-60\%$ of the electric vehicles have between $150-200$ km. While the performance of the material is less than the original, it is clear that a conservative usage is also a viable option. This case is also a viable option when looking for developing vehicles

for urban driving.

In Case 2, with an increased structural battery composite weight, the increased weight of the vehicle still does not completely match the range of the original vehicle. The total range for case 2 (270 km) is around 86% of the original case. It is evident that the two cases, which are built on realistic substitution within the vehicle, are feasible alternatives for using structural battery composites in existing vehicles.

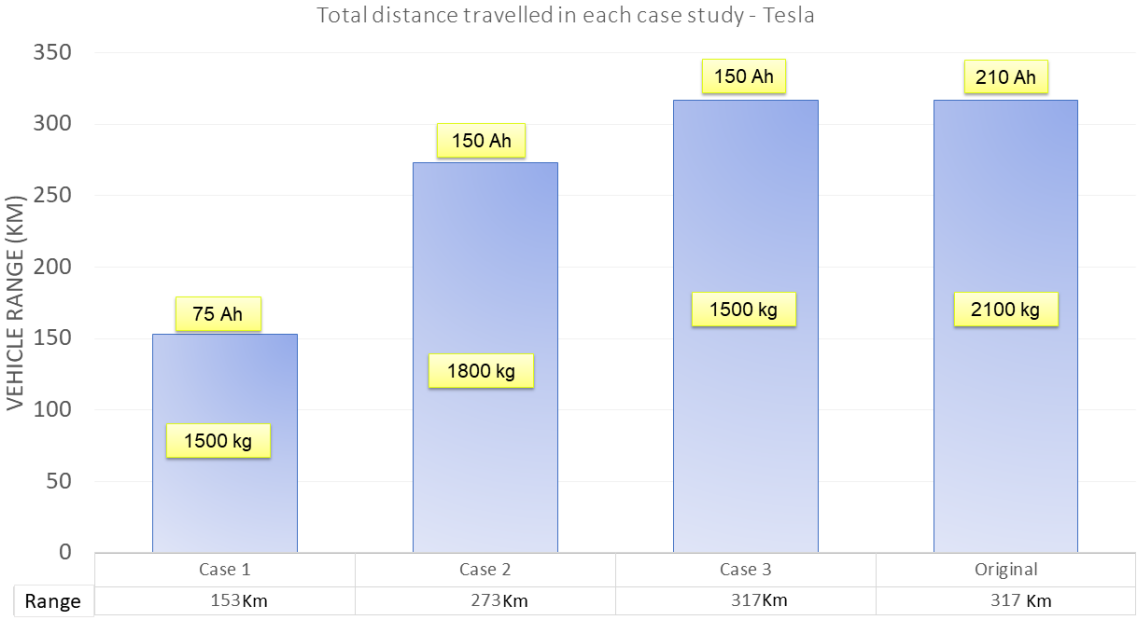

Figure 4.1: The predicted range capacity and mass of the Tesla S

In case 3 the weight of structural battery composite required to maintain the existing range on removing the battery is determine. This is as listed below:

- Weight of of structural battery composite (W_{sbc}): 600 kg
- Total Capacity (C_{sbc}): 150 Ah
- Total vehicle weight (M): 1500 kg

The weight of structural battery used can also be estimated by maintaining the same ratio of vehicle weight to battery capacity. The vehicle weight required in case 3 can be achieved by downsizing components as well as substituting more parts of the vehicle with the structural battery composite compared with case 1. It is also evident that a 30% mass saving is possible upon using structural battery composites in vehicles comparing the weight for the case 3 (1500 kg) with the original weight (2100 kg).

It should be noted that the vehicle weight is identical for case 1 and3 but the range in the later is twice of the former. This is because 600 kg of structural battery composite is assumed to be incorporated within the structure in case 3 while only 300 kg in case 1.

4.1.2 BMW i3

The predicted range for the BMW i3 with the structural battery composite and the original battery is depicted in Figure 4.2. Similar to the analysis performed for the Tesla Model S, case 1 shows a capability good for urban driving. The performance of the first case also matched 60% of existing vehicle range. It is also matched $50-60\%$ of the range from the lower rated variant of the BMW i3 (22 kWh, 60 Ah).

Case 2, predicts a range similar to the rated range of the BMW i3 (22 kWh, 60 Ah). The range also is close to 90% of the original rated range. The results of case 2 again shows that the feasibility of using structural battery composites are high. Case 3, following the same logic as for the Tesla Model S. The total weight savings is around 20% when comparing with the original case. This is because the weight of the vehicle is originally vastly reduced by utilising composites in the life module. Downsizing, might provide additional weight savings.

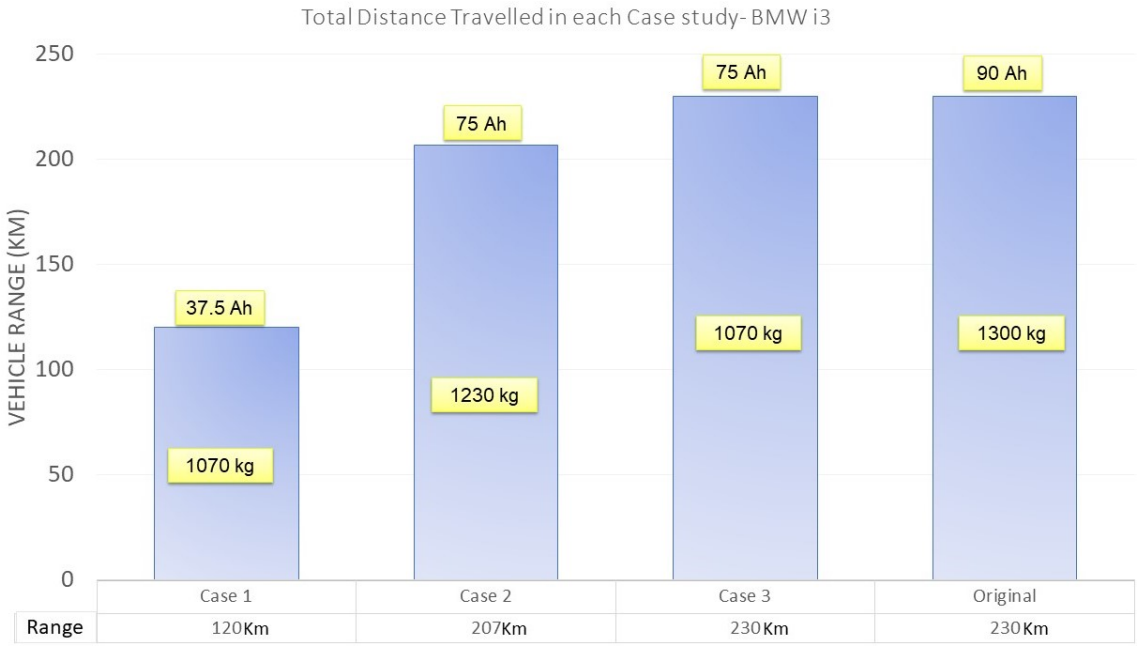

Figure 4.2: The predicted range capacity and mass of the BMW i3

4.1.3 Overall electrical performance

The overall electrical performance is given by the electrical efficiency as depicted in Equation 2.25. Physically, it would be the ratio of useful energy to the total energy available. Because it is divided by the original case, the energy calculation over the velocity cycle can be cancelled. Hence taking only case 3 in the Tesla Model S and BMW i3 to evaluate the electrical performance:

Tesla Model S

$$R_{sbc} = R_{bat} = 317 \qquad M = 2100 \qquad M^* = 1500 \qquad C_{sbc} = 150 \qquad C_{bat} = 210$$
$$\eta^e = \frac{\frac{317 \times 1500}{150}}{\frac{317 \times 2100}{210}} = 1$$

BMW i3

$$R_{sbc} = R_{bat} = 230 \qquad M = 1300 \qquad M^* = 1070 \qquad C_{sbc} = 75 \qquad C_{bat} = 90$$
$$\eta^e = \frac{\frac{230 \times 1070}{75}}{\frac{230 \times 1300}{90}} = 0.987 \approx 1$$

Hence, the electrical performance in the third case for both vehicles have a 100% efficiency.

4.2 Component model

The structural analysis is performed on a exterior door panel of a vehicle. Only the flexural stiffness is evaluated to determine the resistance to oil canning. The FE model was retrieved from Altair's online database [18]. The door was isolated from the model and the door is assumed to be simply supported on all the edges as illustrated in Figure 4.3. A pressure of $20kPa$ is applied over a 10×10 cm area to simulate a hand pressing against the door.

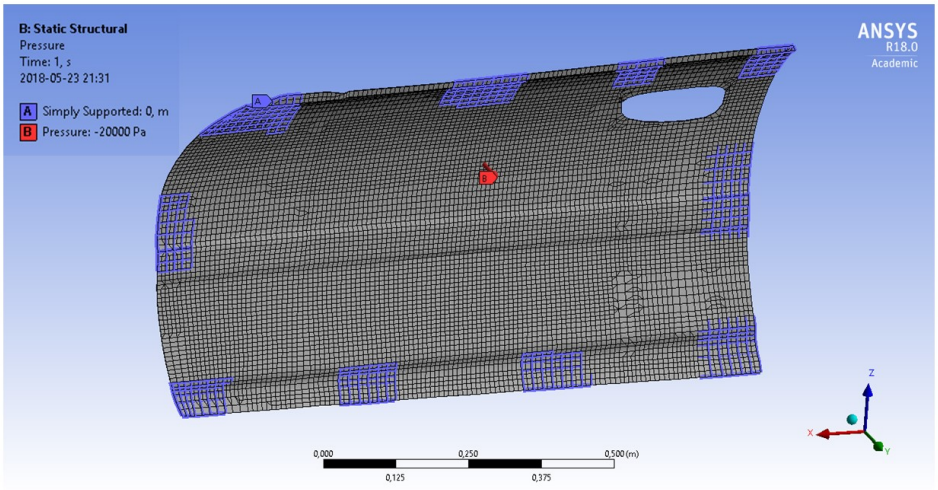

Figure 4.3: Loading conditions of a car door

The considered load case for the exterior door panel is first performed for steel to determine the deformation of the original design under the given load. This helps

in determining the minimum thickness of structural battery composite required to meet the performance of the existing design by having the same maximum deflection.

The door of the vehicle is loaded as discussed earlier. The total deformation experienced using steel is 0.8 mm. The thickness of steel used is 1 mm. This deformation is the requirement on the structural battery composite to meet.

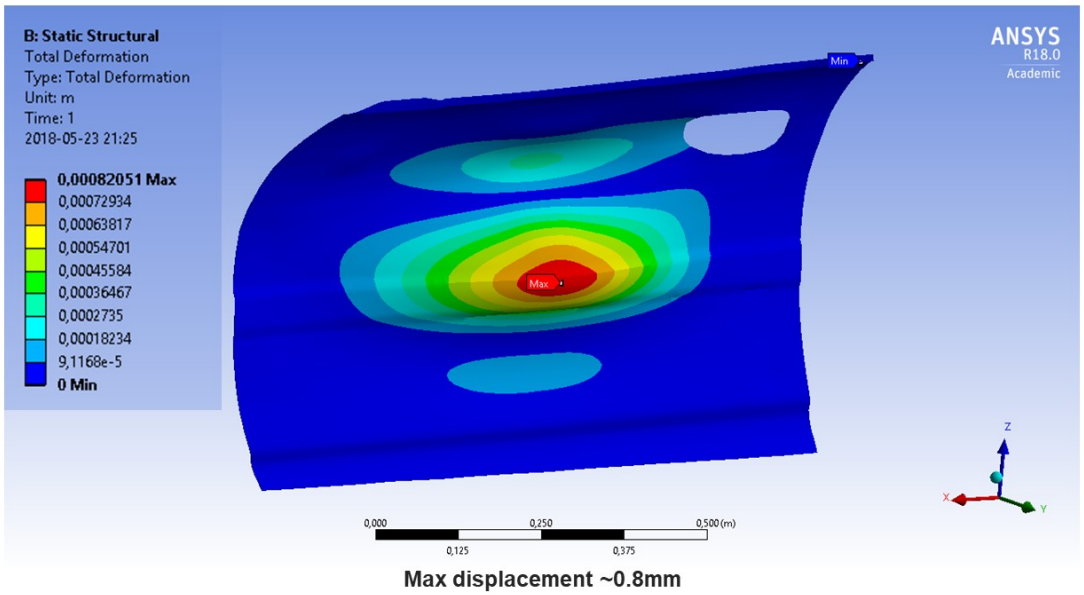

Figure 4.4: Steel door loaded

4.2.1 Deformation

The material was then substituted with the structural battery composite by giving the specific material properties calculated. The thickness of the composite was increased gradually thereby increasing the number of layers. Using a homogenised material property for uni-directional composites(0°) plies the result from gradually increasing the number of plies are summarised in Table 4.1

No. of Layers	Thickness (mm)	Deformation (mm)
1 [0]	0.5	0.85
2 [0/0]	1	10
6 [0/0/0/0/0/0]	3	0.9

Table 4.1: Variation of deformation with thickness number of layer of composite

4.2.2 Thickness and mass variation

The secondary case studies were performed comparing materials that can be used for the vehicle structural components. To provide the same stiffness as that of a

door panel made out of steel, the thickness of structural battery composite is 3 mm. A summary of the properties of the materials is as listed in Table 4.2

Material	Density(g/cm^3)	Thickness (cm)
Steel	7.5	0.85
Structural battery composite	1.5	3

Table 4.2: Material properties and deformation for steel and structural battery composite door panel

Now, considering the same door in both cases, there is only a variation of thickness in terms of dimensions. Hence the overall area (A) will be constant. With a varying thickness and density the mass will vary. Taking the ratio of mass with steel (m_s) and the structural battery composite (m_{sbc}), the weight difference can be calculated. This is depicted in the Equations 4.1-4.5

$$V_i = A \times t_i \tag{4.1}$$

$$M_i = V_i \times \rho_i \tag{4.2}$$

$$W_{save} = 1 - \frac{M_i}{M_j} \tag{4.3}$$

$$\implies W_{save} = 1 - \frac{A \times t_i \times \rho_i}{A \times t_j \times \rho_j} \tag{4.4}$$

$$\implies W_{save} = 1 - \frac{t_i \times \rho_i}{t_j \times \rho_j} \tag{4.5}$$

$$\tag{4.6}$$

It is seen that the volume of the door component using a particular material ($V_i,\ V_j$) is the product of the area and the thickness of the material ($t_i,\ t_j$) used. This volume with the density gives the mass ($m_i,\ m_j$). To calculate the thickness using structural battery composite needed to match the mass of the door panel (in order to meet requirement on capacity) the ratio of weight of door component can be used. The results of this analysis is summarised in Table 4.3

Material	Weight ratio
Steel/structural battery composite	1.3

Table 4.3: Weight comparison between steel and structural battery composite

It is clear that when substituting a steel door with a door panel made out of structural battery composite while assuming the same stiffness there is 30% mass reduction. However, unless the electrical capacity is provided elsewhere the thickness of the structural battery composite need to be increased with the ratio of the weights. in aluminium there is not much weight savings, there is more so weight gains.

4.2.3 Overall structural performance

The structural performance is linked to the amount of structural battery composite used to maintain the structural integrity of the vehicle. Hence, the evaluation of the structural performance of the door panels is given in as :

$$\eta^s = \frac{4 \times (4.5) + \sum_{i=5}^{n}(m_i - m_i^*)}{600} = 0.028 + \sum_{i=5}^{n} \frac{(m_i - m_i^*)}{600}, \tag{4.7}$$

where, 4.5 kg corresponds to the weight allocated to one door component, and m_i corresponds to the other components where the structural battery composite is allocated to maintain the structural integrity of other components. Hence, the structural performance of the structural battery composite when accounting for the door panels starts at 0.03.

4.3 Multi-functional performance

For the overall structural performance, using Equations 2.25-2.27, feasibility of using structural battery composites is possible. This is because, the electrical performance (η^e) is one. When looking at the structural performance (η^s) with one component alone and using steel is 0.03. Hence:

$$\eta^e + \eta^s \approx 1.03 > 1 \tag{4.8}$$

It is important to also note that due to the contribution of only one component among the structural stiffness, 1.03 is the minimum and it will be higher once the structural performance is analysed for all the other components. Given that structural performance is met for all components assumed to be replaced with structural battery composite in the case studies, the sum for case 3 is 1.3 and 1.2 for the Tesla and BMW respectively.

5

Conclusions

It is evident that in battery electric vehicles having mainly metal components, will benefit from potentially 30 percent or more weight savings from using structural battery components. This is possible by just using a multi-functional material as opposed to a mono-functional battery. There can be a further reduction in the weight of the vehicle by downsizing components and other light-weighting strategies. However, while the composite is much lighter, there is also a constraint on the space available which has to be considered when adopting structural battery composites. Furthermore, there is a gap in the predictive model which does not validate if the power required can be delivered by the battery pack. However, the availability of energy, is kept in check based on the depth of discharge.

To truly utilise a holistic design approach for a given vehicle, is to determine the amount of structural battery composite required in a vehicle to meet a required range. Based on this requirement, the mass of the composite can be allocated to various structural components within the vehicle.

Based on the results obtained, it is observed that the maturity of the structural battery composite is achieved in the third case. From an electrical perspective, the measure for performance is based on the range achieved matches that of the existing vehicles on road. Moreover, the structural performance based on just one component exceeds the minimum requirement for maturity i.e. the sum total of each individual performance is greater than one.

It is also observed that to give a quick approximation of how much structural battery composite is required to meet an existing range, around 30 to 40 percent of the vehicle should be made from structural battery composite.

6

Future work

The structural efficiency is evaluated with just one component of the vehicle. A more in-depth analysis of the overall structural stiffness when substituting parts of the structure with structural battery composite can be done by adopting a simple structural surface (SSS)- method [25]. This will address other loading conditions crucial to vehicle development such as bending, torsion, combined bending and torsion, lateral loading ,etc.

The current structural performance within the multi-functional performance is restricted to only one component. This must be done more exhaustively for other structural components within the vehicle. Then only will the total feasibility of using structural battery composite be accurately determined.

From an electrical performance perspective, there is a requirement on the power delivering capability which must be incorporated. This will also give a better understanding of the actual performance of the composite material. To do this, the discharge characteristics along with the effective resistance of one unit of the structural battery composite must be determined experimentally.

There is also a need to partner with the automotive industry from a utility perspective, this includes knowing the exact vehicle details for the input of the electrical performance for a more accurate comparison. Along with this, working on how to compartmentalise the structural battery composite in the vehicle is key to effectively utilise the composite material in a vehicle. This will eventually also talk about the packaging of the composite material. Due to the lower density, the volume would be larger and with the existing constraint on available space will be a key factor in the future.

Bibliography

[1] A. E. Scholz,(2017) Feasibility Analysis and Comparative Assessment of Structural Power Technology in All-Electric Composite Aircraft, Master thesis, Imperial College London.

[2] Asp, Leif & Greenhalgh, Emile. (2014). Structural power composites. Composites Science and Technology. 101. 41–61. 10.1016 j.compscitech.2014.06.020.

[3] J.F. Snyder, E.L. Wong & C.W. Hubbard.(2009). Evaluation of commercially available carbon fibers, fabrics, and papers for potential use in multifunctional energy storage applications. Journal of The Electrochemical Society, 156:A215–A224 .

[4] Ihrner, N., Johannisson, W., Sieland, F., Zenkert, D., Johansson, M. (2017). 'Structural lithium ion battery electrolytes via reaction induced phase-separation'. Journal of Materials Chemistry A, 5(48), 25652-25659.

[5] Carlstedt D (2017). 'Structural Battery Composites'. Course project report, Chalmers University of Technology, Goteborg, Sweden.

[6] T. Carlson,(2013). 'Multifunctional composite materials: Design, manufacture and experimental characterisation', PhD dissertation, Luleå, Sweden.

[7] L.E. Asp, A. Bismarck, T. Carlson, G. Lindbergh, S. Leijonmarck & M. Kjell, (2014). A battery half-cell, a battery and their manufacture. PRV, Patent No. SE537063 C2 Sweden, 2014 (structural battery).

[8] L.E. Asp, A. Bismarck, T. Carlson, G. Lindbergh, S. Leijonmarck & M. Kjell . A battery half-cell, a battery and their manufacture (structural battery). PCT, Patent No. 2893582, November 16th 2016. (Intl Appl No. PCT/EP2013/068024, 2013).

[9] S. Leijonmarck, T. Carlson, G. Lindbergh, L.E. Asp, H. Maples & A. Bismarck, (2013). Solid polymer electrolyte coated carbon fibres for structural and novel micro batteries. Composites Science and Technology, 89:149-157.

[10] E.D. Wetzel. Multifunctional structural composite materials for US Army applications. AMPTIAC Q, 8(4):91–95, 2004.

[11] E.L. Wong, D.M. Baechele, K. Xu, R.H. Carter, J.F. Snyder and E.D. Wetzel. Design and processing of structural composite batteries. Proceedings SAMPE 2007, SAMPE, Baltimore, MD, USA, June 2007.

[12] S. Ekstedt, M. Wysocki and L.E. Asp. Structural batteries made from fibre reinforced composites. Plastics, Rubber and Composites, 39:148–50, 2010.

[13] T. Carlson. Multifunctional composite materials – design, manufacture and experimental characterisation, Doctoral Thesis, Luleå University of Technology, 2013.

[14] Obrien, D. J., Baechle, D. M., Wetzel, E. D. (2011). 'Design and performance of multifunctional structural composite capacitors. Journal of Composite Materials', 45(26), 2797-2809.

[15] Omar, N., Daowd, M., Bossche, P. V., Hegazy, O., Smekens, J., Coosemans, T., Mierlo, J. V. (2012, August 10). Rechargeable Energy Storage Systems for Plug-in Hybrid Electric Vehicles-Assessment of Electrical Characteristics. Retrieved March, 2018, from http://www.mdpi.com/1996-1073/5/8/2952

[16] Larminie, J., Lowry, J. (2012). 'Electric vehicle technology explained'. Chichester: John Wiley and Sons.

[17] Younes, Rafic & Hallal, Ali & Fardoun, Farouk & hage Chehade, Fadi. (2012). Comparative Review Study on Elastic Properties Modeling for Unidirectional Composite Materials. 10.5772/50362.

[18] Altair university. (n.d.). Ready to use 3D Models. Retrieved from https://altairuniversity.com/modeling/model-repository/

[19] D. Carlstedt, W. Johannisson, D. Zenkert, P. Linde and L.E. Asp (2018). Conceptual design framework for laminated structural battery composites. In: Proceedings of the ECCM18. Athens, Greece.

[20] SORCERER - Structural power composites for future civil aircraft, project no. 738085, Clean Sky II, H2020 2017-2020

[21] Network, T. (2014, July 02). Tesla Model S Weight Distribution. Retrieved February 1, 2018, from https://www.teslarati.com/tesla-model-s-weight/

[22] Schaeffler, D. J., Engineering Quality Solutions Inc. (2015, September 14). Sheet aluminum alloys for cans and cars. Retrieved April 22, 2018, from https://www.thefabricator.com/article/metalsmaterials/sheet-aluminum-alloys-for-cans-and-cars

[23] More details on BMW's i3; electric and connected. (2013, July 10). Retrieved February 20, 2018, from http://www.greencarcongress.com/2013/07/bmwi3-20130710.html

[24] Starke, D. J. EuCIA:Composites and Sustainability.(2016,March 19). Retrieved February 20, 2018, from http://www.eucia.eu/userfiles/files/Starke-Eucia 2016-V4-Druck b.pdf

[25] Happian-Smith, J. (2006). An introduction to modern vehicle design. Oxford: Butterworth-Heinemann.

7

Appendix

7.1 MATLAB script for predictive model

7.1.1 Open circuit voltage

```
function E_oc=open_circuit_voltage(DoD,Nocells)
%open circuit voltage
%input DoD– Depth of discarge N–No.of Cells
if DoD<0
    error('DoD < 0');

elseif DoD>1
    error('DoD > 1');

end
%E_oc=370;
E_oc=Nocells*(4-(DoD));
%E_oc = (-349798.1 + (4 - -349798.1)/(1 + (DoD/185.0829)
    ^20.21248))*Nocells;
%E_oc=(4-((4-9)*DoD))*Nocells;381422
%E_oc=(2.15-((2.15-2.00)*DoD))*Nocells;
%E_oc=(4.16-((4.16-3)*DoD))*Nocells;
```

7.1.2 Predictive Model

```
%range calculation
clc
clear all
close all
importfile('Vel')
V=NEDC.Data;
N=length(V); % number of readings


```

```
%Car Dimension Data
M=1600; %mass of vehicle in Kg [2100 1850 1750 1500] 140 for weight of 2 passenger
F_m=1.05; % mass Factor
A_front=2.34; %vehicle Frontal Aread tesla 2.34 i3 0.690
R=0.02; %Internal resistance of one cell
Cd=0.24; %Co.eff of drag tesla 0.24 i3 0.29
M_SBC=600;
if M_SBC==0
        para=74; %no of cells in parallel
        ser=16*6; %number of modules in series 8 modules 12
       R_int=(ser*R)/para;
        Capacity=210; %Ah
       M=2100;
elseif M_SBC>0
       ser=100; %one module or 10 demonstrators in series
       para=M_SBC/(100*0.04); %Mass of SBC in gms /4 volt in each cell in module
       R_int=(ser*R)/para;
       Capacity=para*(0.04*25);
end
Nocells=para*ser;

%Battery data
T=1; %time for discharge cycle
k=1.1; %Peukert co.eff CHECK
Pax=100; %Ancillary systems power CHECK

%Transimission data
Gratio=20.33; %G=9.75  r=0.48 m both cases is radius of wheel check*
M_eff=0.95;% Motor Efficiency
regen_ratio=0.5; %Regenerative braking ratio

%Motor Losses
Cu_loss=0.3; %Copper Losses
Fe_loss=0.01; %Iron losses
wind_loss=0.000005; %Windage Loss
Cons_elec_loss=600; %Constant electric loss

%Environment data
C_rr=0.02; %Co.eff of rolling resistance
rho=1.225; %Air density kg/m3
V_w=0; %wind speed
theta=0; %road slope angle
g=9.814; %gravitational constant
```

```
53
54 % calculated constants
55 R_int=R_int+0.05; %Allowance for connecting leads
56 C_p=((Capacity/T)^k)*T; %Peukert Capacity c_p=(I^k)*T
57
58
59 %% Initilizing variables
60 %setting to zero for n cycles
61 n=1; %to count number of velocity cycles
62 Dod = zeros(1,n); %End of cycle Depth of Discharge
63 CR = zeros(1,n); %end of cycle charge removed
64 Dist = zeros(1,n); %Distance travelled end of cycle
65
66 %Arrays for within one velocity cycle
67 Dod_V= zeros(1,N); %Depth of Discharge within cycle
68 CR_V= zeros(1,N); %charge removed within cycle
69 Dist_V = zeros(1,N); %Distance travelled within cycle
70 accel=zeros(1,N);
71 Pmot_in=zeros(1,N);
72
73 %% Running cycle
74 C_loop=2; %counter for number of cycles run
75 DoD=0; %Starting DoD and 0% therefore battery at full charge
76 while DoD<0.9
77    %vel_cycle simulates one velocity cycle
78 for C=2:N
79     accel(C-1)=(V(C)-V(C-1))/0.5;
80     Fr=M*g*C_rr*cos(theta)+(1/2)*rho*A_front*Cd*(V(C)-V_w)
         ^2+M*g*sin(theta); %total rolling resistance
81     Ft=F_m*M*accel(C-1)+Fr; %total Traction Force or braking
         force
82     Pte=Ft*V(C); %Propulsion Power or Braking Power
83     omega=Gratio*V(C);
84     if omega==0 %for stationary condition
85         Pte=0;
86         Pmot_in(C-1)=0;
87         Torque=0;
88         eff_mot=0.5; %% check why not zero
89     elseif omega>0 %moving condition
90        if Pte < 0
91        Pte=regen_ratio*Pte;%energy requirement red. as the
            whole o/p not motor
92        pmot_out=Pte*M_eff; %%check this line 283 pg
93        elseif Pte >=0
94        pmot_out=Pte/M_eff;
95        end
```

```
96          Torque=pmot_out/omega;
97          if    Torque>0
98          eff_mot=((Torque)*omega)/(((Torque)*omega)+((Torque)
                ^2*Cu_loss)+...
99                (omega*Fe_loss)+((omega^3)*wind_loss)+
                    Cons_elec_loss);
100       elseif Torque<0
101         eff_mot=((-Torque)*omega)/(((-Torque)*omega)+((Torque
                )^2*Cu_loss)+...
102               (omega*Fe_loss)+((omega^3)*wind_loss)+
                    Cons_elec_loss);
103       end
104           if pmot_out>=0
105               Pmot_in(C-1)=pmot_out/eff_mot;
106           elseif pmot_out<0
107               Pmot_in(C-1)=pmot_out*eff_mot;
108           end
109       end
110       Pbat=Pmot_in(C-1)+Pax;
111       E=(open_circuit_voltage(Dod_V(C-1),ser));
112       if Pbat>0
113            I=(E-(E*E-(4*R_int*Pbat))^0.5)/(2*R_int);
114           CR_V(C)=CR_V(C-1)+(abs(I^k)*0.5/3600);
115       elseif Pbat==0
116            I=0;
117
118       elseif Pbat<0
119            Pbat=-1*Pbat;
120            I=(-E+(E*E+(4*2*R_int*(Pbat)))^0.5)/(2*2*R_int); %
                  guess because rint on charging increased by 2
121           CR_V(C)=CR_V(C-1)-((I)*0.5/3600);
122       end
123       Dod_V(C)=CR_V(C)/C_p;
124       if Dod_V(C)>1
125            Dod_V(C)=1;
126
127       end
128
129     Dist_V(C)=Dist_V(C-1)+(V(C)*0.5/1000); %Dist in km/hr
130
131 end
132     %updating values for end of cycle
133       Dod(C_loop) = Dod_V(N);
134       CR(C_loop) = CR_V(N);
135       Dist(C_loop)=Dist_V(N);
136 %       %carrying over end values for next cycle
```

```
137         Dod_V(1)=Dod_V(N);
138         CR_V(1)=CR_V(N);
139         Dist_V(1)=Dist_V(N);
140         DoD=Dod(C_loop); %carrying over depth of discharge
141         C_loop=C_loop+1;
142
143 end
144 plot(Dist,Dod);
145 ylabel('depth of discharge')
146 xlabel('distance')
```

7.2 Detailed tear-down analysis

7.2.1 Tesla Model S

Weight Analysis	%	Weight Analysis (Kg)
Battery	**28.57**	**600.642**
Al space frame	**17.29**	**363.2**
Motor or drivetrain	**23.23**	**465.35**
electric motor+inverter	34%	158.9
differential	17%	79.45
wheels+tires	24%	113.5
brake calipers disc,lines	12%	54.48
Air susp	8%	36.32
Rack and pinion	5%	22.7
Electrical	**3.67**	**99.88**
wiring , lighting	55%	54.48
Electronics+computer	23%	22.7
HVAC	23%	22.7
Interior	**14.26**	**299.64**
front powered seats+rear	30%	90.8
Windshield,windows,hatch	29%	86.26
Pano glass+assembly	23%	68.1
carpet+padding+mats	12%	36.32
dash+trim+panels	6%	18.16
Exterior	**4.32**	**90.8**
Misc	**8.64**	**181.6**
Total		**2101.112**

Figure 7.1: Tesla Model S tear-down analysis

7.2.2 BMW i3

System	Percentage	Weight Analysis(Kg)
Battery Pack	**17.49%**	**230.00**
Life Module	**10.65%**	**140.00**
FRP	48.93%	68.5
Thermoplastics	9.50%	13.3
Elastomers	0.50%	0.7
AL sheets	10.57%	14.8
Alsheets 2	0.79%	1.1
Al profiles	3.86%	5.4
Cast Al	3.86%	5.4
Mild Steel	7.21%	10.1
Adhesive and foam	13.93%	19.5
Motor or drivetrain	**36.50%**	**479.975**
electric motor+inverter	34.15%	163.8939024
differential	17.07%	81.94695122
wheels+tires	24.39%	117.0670732
brake calipers disc,lines	11.71%	56.19219512
Air susp	7.80%	37.46146341
Rack and pinion	4.88%	23.41341463
Electrical	**6.00%**	**78.9**
wiring , lighting	54.55%	43.03636364
Electronics+computer	22.73%	17.93181818
HVAC	22.73%	17.93181818
Interior	**14.26%**	**187.519**
front powered seats+rear	30.30%	56.82393939
Windshield,windows,hatch	28.79%	53.98274242
Pano glass+assembly	22.73%	42.61795455
carpet+padding+mats	12.12%	22.72957576
dash+trim+panels	6.06%	11.36478788
Exterior	**4.32%**	**56.808**
Misc	**10.64%**	**139.916**
Total	**100.00%**	**1315**

Figure 7.2: BMW i3 tear-down analysis